Robust Hollow Spheres Consisting of Alternating Titania Nanosheets and Graphene Nanosheets with High Photocatalytic Activity for CO_2 Conversion into Renewable Fuels

Wenguang Tu, Yong Zhou, Qi Liu, Zhongping Tian, Jun Gao, Xiaoyu Chen, Haitao Zhang, Jianguo Liu, and Zhigang Zou**

Robust hollow spheres consisting of molecular-scale alternating titania ($Ti_{0.91}O_2$) nanosheets and graphene (G) nanosheets are successfully fabricated by a layer-by-layer assembly technique with polymer beads as sacrificial templates using a microwave irradiation technique to simultaneously remove the template and reduce graphene oxide into graphene. The molecular scale, 2D contact of $Ti_{0.91}O_2$ nanosheets and G nanosheets in the hollow spheres is distinctly different from the prevenient G-based TiO_2 nanocomposites prepared by simple integration of TiO_2 and G nanosheets. The nine times increase of the photocatalytic activity of G-$Ti_{0.91}O_2$ hollow spheres relative to commercial P25 TiO_2 is confirmed with photoreduction of CO_2 into renewable fuels (CO and CH_4). The large enhancement in the photocatalytic activity benefits from: 1) the ultrathin nature of $Ti_{0.91}O_2$ nanosheets allowing charge carriers to move rapidly onto the surface to participate in the photoreduction reaction; 2) the sufficiently compact stacking of ultrathin $Ti_{0.91}O_2$ nanosheets with G nanosheets allowing the photogenerated electron to transfer fast from the $Ti_{0.91}O_2$ nanosheets to G to enhance lifetime of the charge carriers; and 3) the hollow structure potentially acting as a photon trap-well to allow the multiscattering of incident light for the enhancement of light absorption.

1. Introduction

Graphene (G), a 2D sheet of sp^2-hybridized carbon,[1] has drawn considerable attention for fabricating inorganic composites in recent years due to its high thermal conductivity,[2] unique carrier mobility,[3] high flexible structure,[4] high transparency,[5] and large surface area.[6] There is a significant drive within the scientific community to explore its technological applications, such as novel carbon materials,[7] electronics,[6,8] drug delivery,[9] and catalysis.[10] G can be derived from graphene oxide (GO) by heat reduction with microwave irradiation, which can easily restore sp^2 hybridization to yield graphene.[11]

Titania (TiO_2) is a classic wide bandgap semiconductor material that has been widely applied in the field of energy conversion[12] and photocatalysis[13] because of its effectiveness, nontoxicity, low cost, and chemical stability. Numerous photocatalytic applications for TiO_2 have been studied, including pollutant degradation,[13] water photolysis,[14] and carbon dioxide (CO_2) reduction.[15] During the photocatalytic process, the effective electron–hole pairs are generated when the electrons are excited from the valence band of TiO_2 to the conduction band with the photoabsorption.[16] However, effective electron–hole pairs can be recombined and dissipated as heat easily before they arrive at the photocatalyst surface, which limits its efficiency of photocatalytic activity.[17]

Dr. W. Tu, Prof. Y. Zhou, Dr. Z. Tian, Dr. J. Gao, Dr. X. Chen, Prof. Z. Zou
School of Physics
Nanjing University
Nanjing 210093, P. R. China
E-mail: zhouyong1999@nju.edu.cn; zgzou@nju.edu.cn

Dr. W. Tu, Prof. Y. Zhou, Dr. Q. Liu, Dr. Z. Tian, Dr. J. Gao, Dr. J. Liu, Prof. Z. Zou
Eco-materials and Renewable Energy Research Center (ERERC)
Nanjing University
Nanjing 210093, P. R. China

Prof. Y. Zhou, Dr. J. Liu, Prof. Z. Zou
National Laboratory of Solid State Microstructures
Nanjing University
Nanjing 210093, P. R. China

Dr. Q. Liu, Dr. X. Chen, Dr. J. Liu, Prof. Z. Zou
Department of Materials Science and Engineering
Nanjing University
Nanjing 210093, P. R. China

Dr. Q. Liu
School of Mechanical and Automotive Engineering
Anhui Polytechnic University
Wuhu 241000, P. R. China

Dr. H. Zhang
CAS Key Lab of Green Process & Engineering
Institute of Process Engineering
Chinese Academy of Sciences
Beijing100190, P. R. China

DOI: 10.1002/adfm.201102566

To improve efficiency of TiO_2 photocatalytic activity, carbon materials such as carbon nanotubes[18] are used to synthesize carbon-based nanocomposites. In particular, considerable work has been reported about G-based TiO_2 nanocomposites due to its unique properties listed above.[19–30] These works focus on different aspects such as the approach for synthesis of G-based TiO_2 composites,[19–21] the photocatalytic reduction of GO by TiO_2,[22–24] the degradation of organic contaminants,[25–27] and water photolysis.[28,29] To date, photocatalytic conversion of CO_2 to valuable hydrocarbons using solar energy has attracted a great deal of attention because it is one of the best solutions to both the global warming and the energy shortage problems. Nevertheless there is little reported about utilizing G-based TiO_2 nanocomposites for photocatalytic CO_2 conversion into renewable fuel.[31]

Here, we report the assembly of titania ($Ti_{0.91}O_2$) nanosheets and GO nanosheets onto poly (methyl methacrylate) (PMMA) beads via a layer-by-layer (LBL) method to fabricate hollow spheres consisting of alternating $Ti_{0.91}O_2$ nanosheets and G nanosheets for high efficiency photocatalytic applications. The highly crystalline titania nanosheets are of extremely high 2D anisotropy with lateral dimensions of 0.1–1μm and a thickness of ≈0.75 nm.[32] Microwave irradiation allows simultaneously rapid heat reduction of GO nanosheets[11] and the removal of the PMMA template. The molecular scale, 2D contact of $Ti_{0.91}O_2$ nanosheets and G nanosheets in the hollow spheres is distinctly different from the previously reported G-based TiO_2 nanocomposites prepared by the simply integration of TiO_2 and G nanosheets.[19,27] The higher photocatalytic activity of G-$Ti_{0.91}O_2$ hollow spheres was investigated by photocatalytic CO_2 conversion. The nine-times enhancement of the photocatalytic activity relative to commercial P25 results from: 1) the ultrathin nature of $Ti_{0.91}O_2$ nanosheets allowing charge carriers to move rapidly onto the surface; 2) the sufficiently compact stacking of ultrathin $Ti_{0.91}O_2$ nanosheets with G nanosheets enabling the photogenerated electron to fast transfer from $Ti_{0.91}O_2$ nanosheets to G to enhance lifetime of the charge carriers; and 3) the hollow structure potentially acting as a photon trap well to allow the multiscattering of incidence light for the enhancement of light absorption.

2. Results and Discussion

The overall fabrication procedure of the hollow sphere consisting of alternating $Ti_{0.91}O_2$ nanosheets and G nanosheets is schematically illustrated in **Figure 1**. Based on LBL assembly procedures, poly(methly methacrylate) (PMMA) spheres were successively modified with a protonic polyethylenimine (PEI) aqueous solution (Figure 1a), a colloidal suspension of negatively charged $Ti_{0.91}O_2$ nanosheets (Figure 1b), a protonic PEI aqueous solution (Figure 1c), and a negatively charged GO suspension (Figure 1d). Due to the electrostatic attraction between them, the building sheets were adsorbed onto the surface of the PMMA templates to form core/shell composites. Every deposition step involved dispersing, mixing, centrifuging, washing, and re-dispersing operations. After repeating the dipping cycles several times, the yellow-brown composites with five layers of $(PEI/Ti_{0.91}O_2/PEI/GO)_5$ were obtained (Figure 1e). The coated

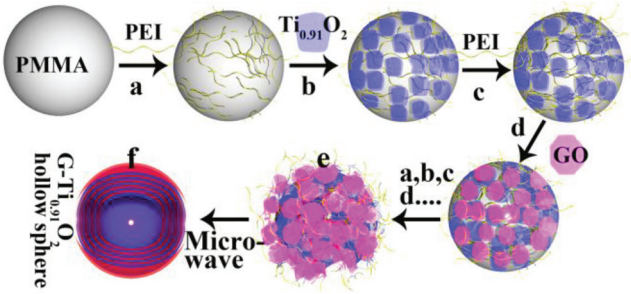

Figure 1. Schematic illustration of procedure for preparing the LBL-assembled multilayer-coated spheres consisting of titania nanosheets and GO nanosheets, followed by microwave reduction of GO into G.

PMMA was then placed in a crucible surrounded with carbon powder with property of strong microwave absorption. The color of the yellow-brown $(PEI/Ti_{0.91}O_2/PEI/GO)_5$ changed to black (Figure 1f and **Figure 2**) and its weight decreased more than 80% after microwave irradiation in argon (Ar) atmosphere, indicating that GO was reduced to G, the PEI moiety was removed, and the PMMA spheres as sacrificial templates were decomposed into exhaust gas. The remaining trifle PMMA residue can be completely removed with tetrahydrofuran.

The field emission scanning electron microscopy (FE-SEM) images reveal the noteworthy rough texture of the spherical surface of the GO and titania nanosheet-coated PMMA (**Figure 3**b), compared with the smooth surface of a bare PMMA sphere that exhibits no any notable features (Figure 3a). Partial GO patch peeling off from the core surfaces and corrugation can clearly be observed. It proves the block sheets have indeed been successfully coated onto PMMA. With microwave irradiation, local high temperature resulted in rapid decomposition of the PMMA core into exhaust gas to generate hollow structures (Figure 3d). Some occasional holes and traces of rupture of the microwave-treated nanocomposites prove the production of hollow spheres, as indicated with arrows. The well preserved spherical configuration after removal of the template demonstrates the robust virtue of the hollow spheres.

Corresponding transmission electron microscopy (TEM) images of $(PEI/Ti_{0.91}O_2/PEI/GO)_5$ coating on the PMMA beads show the existence of the thin nanosheets with wrinkles

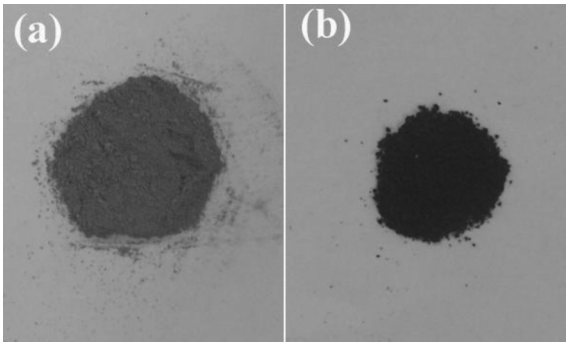

Figure 2. Photographs of PMMA spheres coated with $(PEI/Ti_{0.91}O_2/PEI/GO)_5$ a) before and b) after microwave irradiation.

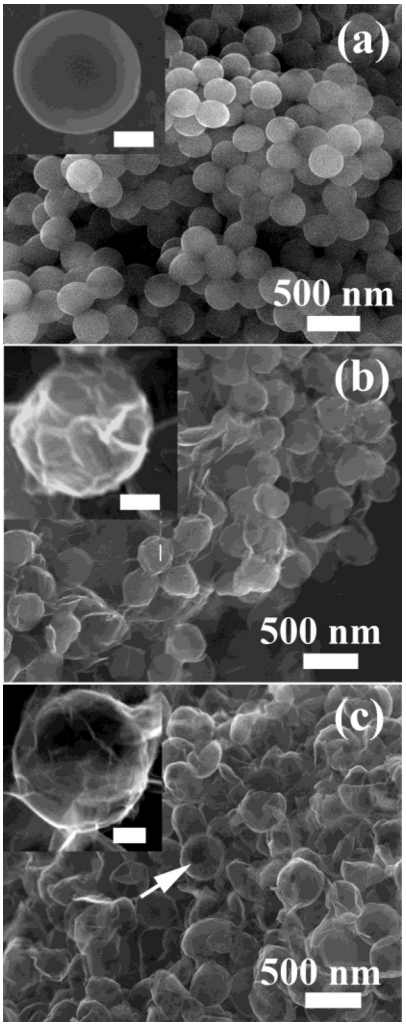

Figure 3. FE-SEM images of a) bare PMMA spheres, b) PMMA spheres coated with $(PEI/Ti_{0.91}O_2/PEI/GO)_5$, and c) $(G\text{-}Ti_{0.91}O_2)_5$ hollow spheres. Scale bars of the insets: a,b) 100 nm and c) 250 nm.

and folds (**Figure 4**a). The parallel-aligned dark lines indicate the layered structure of the GO-$Ti_{0.91}O_2$ shell (Figure 4b). With microwave irradiation for the removal of PMMA, TEM clearly reveals the hollow structure of the resulting sphere (Figure 4c). High-magnification TEM observation reveals intactness of the multilayer stacking structures of alternatively $Ti_{0.91}O_2$ nanosheets and reduced GO nanosheets (Figure 4d), resembling lamellar fringes. The lamellar fringes are completely parallel, which is consistent with the LBL assembly of the alternative two nanosheets. A fast Fourier transformation (FFT) pattern also indicates highly ordered lamellar structures (inset of Figure 4d).

The structural order in the multilayer-coated PMMA with $(PEI/Ti_{0.91}O_2/PEI/GO)_5$ before and after microwave irradiation were demonstrated using X-ray diffraction (XRD) patterns (**Figure 5**). The broad peak centered at 15° can be assigned to amorphous phase of PMMA. Compared with the XRD of bare PMMA spheres (Figure 5a), the as-prepared multilayer-coated PMMA with $(PEI/Ti_{0.91}O_2/PEI/GO)_5$ shows a diffraction peak at

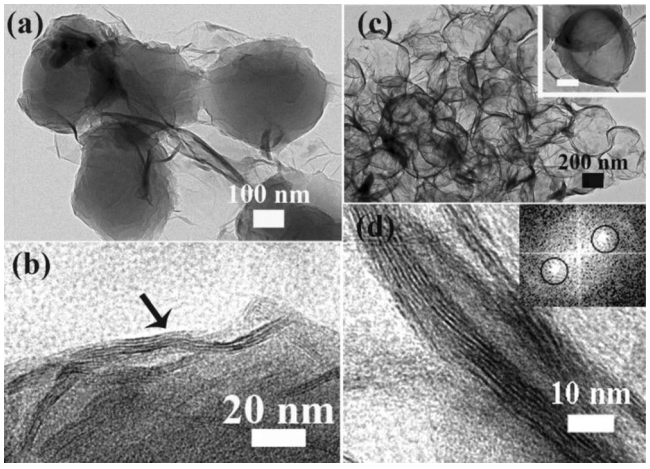

Figure 4. TEM images of a,b) PMMA spheres coated with $(PEI/Ti_{0.91}O_2/PEI/GO)_5$, c,d) $(G\text{-}Ti_{0.91}O_2)_5$ hollow spheres. Scale bar of the inset in (c): 100 nm.

$2\theta = 5.3°$ (Figure 5b), ascribed to (010) reflections of the lamellar nanostructures, which suggests successful assembly of the repeated inorganic-organic layers of $PEI/Ti_{0.91}O_2/PEI/GO$ on PMMA surfaces. The $Ti_{0.91}O_2$ nanosheets and GO nanosheets alternate in a parallel arrangement, with a repeating distance of about 1.608 nm. A distance change in the peak location was contracted to 7.6° after microwave irradiation, and the corresponding repeating distance is reduced to 1.15 nm, which can be attributed to the loss of the oxide groups from GO and the removal of the PEI moiety. Decrease of the repeating distance suggests that the interlays are stacked more compactly.

Figure 6 compares the Raman spectra of PMMA spheres with $(PEI/Ti_{0.91}O_2/PEI/GO)_5$ before and after microwave irradiation. Both spectra show the existence of two peaks, D band and G band of the carbon species. The G mode is related to

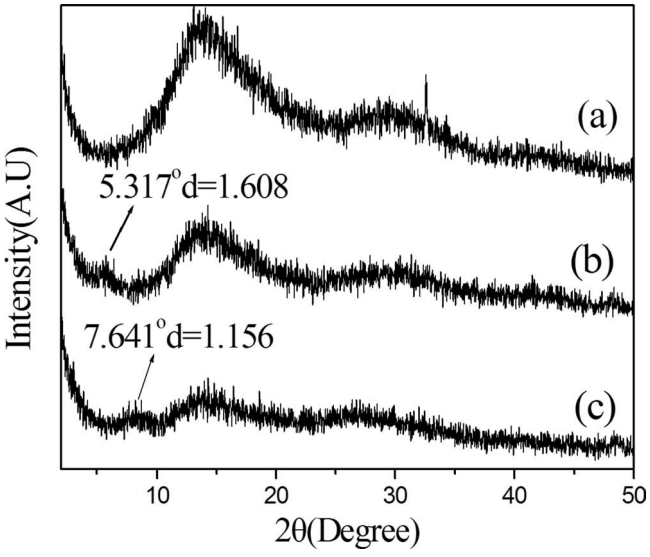

Figure 5. XRD patterns of core/shell composites: a) bare PMMA spheres, b) PMMA spheres coated with $(PEI/Ti_{0.91}O_2/PEI/GO)_5$, and c) $(G\text{-}Ti_{0.91}O_2)_5$ hollow spheres.

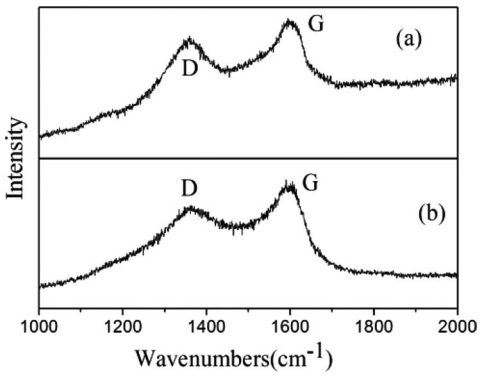

Figure 6. Raman spectra of a) PMMA spheres coated with $(PEI/Ti_{0.91}O_2/PEI/GO)_5$ and b) $(G\text{-}Ti_{0.91}O_2)_5$ hollow spheres.

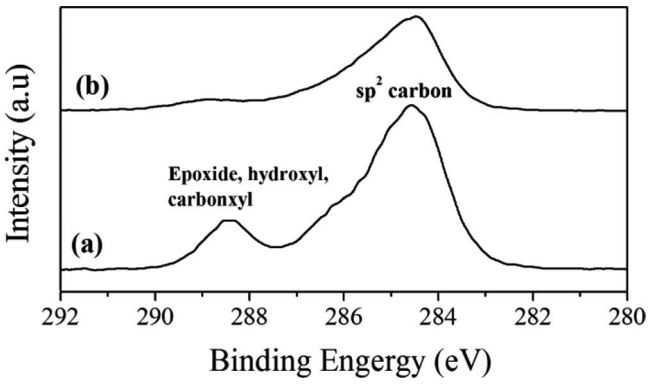

Figure 8. C 1s XPS spectra of a) PMMA spheres coated with $(PEI/Ti_{0.91}O_2/PEI/GO)_5$ and b) $(G\text{-}Ti_{0.91}O_2)_5$ hollow spheres.

the vibration of sp^2-hybridized carbon with the π states.[34] It is notable that the G band peak is located at a higher frequency in the as-prepared samples than in the samples after microwave irradiation (1594.1 versus 1588.6 cm^{-1}). The shift of the G band in GO is usually attributed to the presence of isolated double bonds that resonate at higher frequencies than the G band of graphite.[33–35] The latter is close to the value of the pristine graphite, which indicates the increase of sp^2-hybridized carbon. Meanwhile, the existence of the D band at 1359.1 and 1365.1 cm^{-1} for the samples before and after microwave irradiation, respectively, shows the defect of the in-plane sp^2 domain.[34] The intensity ratio of the D band to G band, $I(D)/I(G)$, changes from 0.91 to 0.85 due to the removal of hydroxyl and epoxy groups and the restoration of sp^2-hybridized carbon with microwave irradiation.

A Fourier-transform infrared (FTIR) spectroscopy study analyzed reduction of GO nanosheets and removal of the PMMA polymer (**Figure 7**). The characteristic absorption of PMMA is derived from C–H stretching vibration of CH_2 and CH_3 group (2800–3000 cm^{-1}), C–H bending vibration (1388 cm^{-1}, 1484 cm^{-1}), C=O stretching vibration (1730 cm^{-1}), and C–O–C stretching vibration (1150 cm^{-1}, 1194 cm^{-1}, 1243 cm^{-1}, 1271 cm^{-1}) (Figure 7a).[36] For the hollow sphere, the characteristic absorptions of PMMA almost disappear, which confirms the successful removal of polymers (Figure 7b). The characteristic absorption bands of GO[37] (970 cm^{-1} for epoxy stretching, 1060 cm^{-1} for C–O stretching, and 1220 cm^{-1} and 1370 cm^{-1} for C–OH stretching) are also absent, and the skeletal vibration of G nanosheets at 1582 cm^{-1} attributed to the aromatic C=C group appearance.[38] This suggests that GO was mainly reduced to G. The disappearance of the broad absorption at 3000–3700 cm^{-1} assigned to O–H stretching vibrations is related to removal of absorbed water after microwave irradiation. The X-ray photoelectron spectroscopy (XPS) data show a significant decrease of oxygenated carbon related signals at 286–289 eV after microwave irradiation (**Figure 8**b), confirming that most of the epoxide, hydroxyl, and carboxyl functional groups were successfully removed and GO was converted to G.

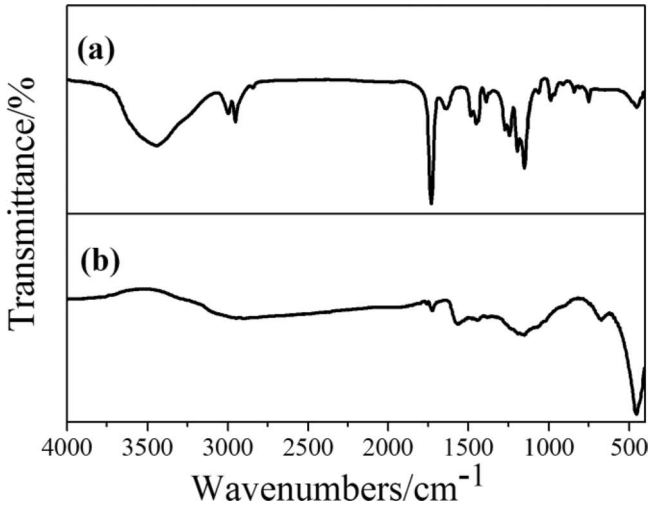

Figure 7. FTIR spectra of a) PMMA spheres coated with $(PEI/Ti_{0.91}O_2/PEI/GO)_5$ and b) $(G\text{-}Ti_{0.91}O_2)_5$ hollow spheres.

To evaluate the photocatalytic activity of $G\text{-}Ti_{0.91}O_2$ hollow spheres, the photocatalytic CO_2 conversion in the presence of water vapor was investigated. Many studies have demonstrated that CH_4 and CO were detected as the major product of CO_2 photocatalytic reduction.[39] CO was the major product and a relatively small amount of CH_4 was obtained on the $G\text{-}Ti_{0.91}O_2$ hollow spheres with a rate of 8.91 μmol g^{-1} h^{-1} and a rate of 1.14 μmol g^{-1} h^{-1}, respectively (**Figure 9**a). Blank experiment with identical condition and in the absence of CO_2 shows no appearance of CH_4 or CO, proving that the carbon source was completely derived from the input CO_2. In the case of $(Ti_{0.91}O_2)_5$ hollow spheres as a photocatalyst, CH_4 was observed as an exclusive product with a rate of 1.41 μmol/g·h, and CO was not detected (Figure 9b). The total yield conversion of CO_2 of $G\text{-}Ti_{0.91}O_2$ hollow spheres exhibit five-times higher than $Ti_{0.91}O_2$ hollow spheres (Figure 9d), which demonstrates it is quite effective to employ G for improving efficiency of $Ti_{0.91}O_2$ photocatalytic activity. The plausible reason is that upon bandgap excitation of $Ti_{0.91}O_2$ nanosheets, holes and electrons are generated in the valence band and the conduction band, respectively. The electrons and holes either take part in redox reactions at the surface or recombine, and the recombination process has faster kinetics than the redox reactions. The presence of G nanosheets compactly stacking with $Ti_{0.91}O_2$ nanosheets allows the photogenerated electron to migrate fast

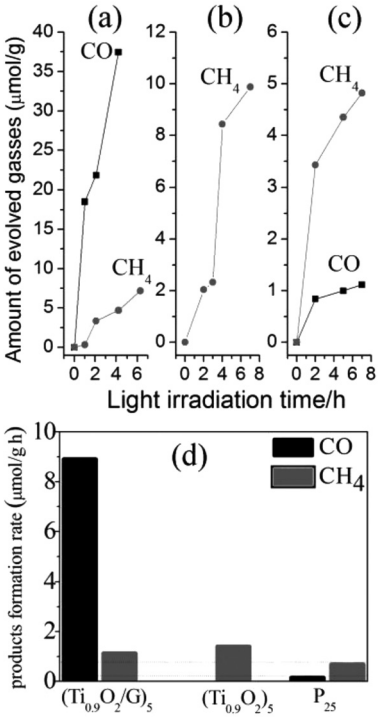

Figure 9. Photocatalytic CH_4 (dots) and CO (squares) evolution amounts for a) $(G\text{-}Ti_{0.91}O_2)_5$ hollow spheres, b) $(Ti_{0.91}O_2)_5$ hollow spheres, and c) P25. d) Comparation of the average product formation rates.

from $Ti_{0.91}O_2$ nanosheets into G, leading to the spatial separation of the electrons and holes. It thus enhances lifetime of the charge carriers and therefore improves the efficiency of the photocatalytic process. The efficient charge transfer in the case of $Ti_{0.91}O_2$/G may originate from the surface conjugation (d–π conjugate) of titania with G. While the $Ti_{0.91}O_2$ hollow spheres show a broad photoluminescence (PL) emission band similar to $Ti_{0.91}O_2$ colloidal solution,[40] a decrease in the PL intensity of $Ti_{0.91}O_2$ hollow spheres after hybridization proves depression of electron–hole recommendation (**Figure 10**). As a comparison, CH_4 and CO was obtained with commercial P25 TiO_2 as catalyst with rates of 0.69 μmol g^{-1} h^{-1} and 0.16 μmol g^{-1} h^{-1}, respectively, indicating that the photocatalytic activity of P25 is lower than that of $Ti_{0.91}O_2$ hollow spheres. The higher photocatalytic activity of $Ti_{0.91}O_2$ hollow spheres may be caused by its surface area for chemical reaction, which better employs its special advantage of separate reduction sites (edge) and oxidation sites (surface),[41] and its ultrathin thickness, which allows charge carriers to move rapidly onto the surface to participate in the photoreduction reaction. In addition, the hollow structure may also act as a photon trap-well to allow the multiscattering of incidence light for the enhancement of light absorption. With regard to generation of different products, i.e., CO and CH_4, via two-electron and eight-electron transfer processes, respectively, the generation of CH_4 is a major product over titania catalyst through the reaction route: $CO_2 \rightarrow CO \rightarrow C\cdot \rightarrow CH_2 \rightarrow CH_4$.[15,39] In the $G\text{-}Ti_{0.91}O_2$ hollow sphere system, CO was dominantly produced. The possible reason may be explained as following: the transferred electrons to G diffuse

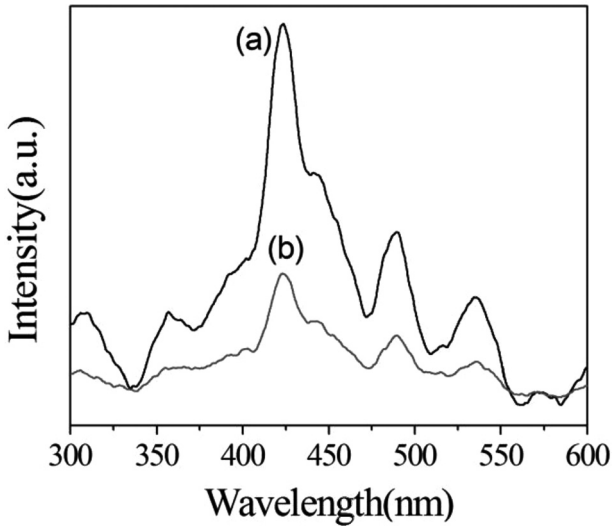

Figure 10. PL emission spectra of a) $(Ti_{0.91}O_2)_5$ hollow spheres and b) $(G\text{-}Ti_{0.91}O_2)_5$ hollow spheres.

quickly on a larger area of G, befitting from the enhanced electrical mobility of G. This restrains the accumulation of the electrons and decrease local electron density, which is favorable for two-electron interaction to form CO.

3. Conclusions

We have successfully fabricated novel hollow spheres consisting of molecular-scale alternating $Ti_{0.91}O_2$ nanosheets and G nanosheets via combination of the LBL assembly technique and a microwave irradiation technique. The structure and combination of $Ti_{0.91}O_2$ nanosheets and G nanosheets lead significant enhancement of the lifetime of electron–hole pair photogenerated from $Ti_{0.91}O_2$ nanosheets upon light irradiation. $G\text{-}Ti_{0.91}O_2$ hollow spheres prove to be an efficient photocatalyst for CO_2 conversion in the presence of water vapor. This work provides a novel method for the improvement of photocatalytic activity. We anticipate that this novel G-titania nanocomposite may also be useful in other fields, such as dye-sensitized solar cells, supercapacitors, and sensors.

4. Experimental Section

Materials: PMMA spheres had an average diameter of 0.3 μm. PEI, a cationic polyelectrolyte, was purchased from Alfa Aesar and used as received. $Ti_{0.91}O_2$ nanosheets were prepared using a previously reported method.[32] GO nanosheets were prepared using a modified Hummer's method from graphite powders.[33] The obtained GO nanosheets were dispersed in deionized water by ultrasonic treatment prior to being used in the experiment.

Fabrication Procedure for Hollow Shells Consisting of Alternating Titania Nanosheets and G Nanosheets: Core/shell composites employing PMMA spheres as templates were fabricated via the LBL self-assembly approach using GO nanosheets and $Ti_{0.91}O_2$ nanosheets as inorganic shell building blocks. PEI, an effective disperser in aqueous solution, was utilized to modify the surface of PMMA spheres. The detailed fabrication procedure of hollow shells is as follows. 1 g of PMMA spheres were dispersed in 200 mL of deionized water containing 0.5 g of PEI at pH 9.0 under

stirring to introduce positive charges to the surface of PMMA spheres. Dilute HCl or ammonia solutions were used to adjust the pH. The suspension was then ultrasonically treated for 10 min. Further stirring was carried out for another 15 min to ensure the saturated adsorption of PEI on the surface of the PMMA spheres. The excess PEI was removed by two centrifugation (8000 rpm at 17% for 5 min) and wash cycles. Afterward, the PEI-coated PMMA was dispersed in 200 mL of deionized water at pH 9.0 and ultrasonically treated for another 10 min. A portion of the colloidal suspension of negatively charged $Ti_{0.91}O_2$ nanosheets at pH 9.0 was added to the turbid PMMA suspension under stirring until the supernatant was almost transparent and the resulting product was sedimented due to the electrostatic interaction of the oppositely charged nanosheets and PMMA surface. Finally, the resulting material was recovered by a separation and washing process, and the excess $Ti_{0.91}O_2$ nanosheets were removed simultaneously. The above procedure was repeated until five bilayers of $(PEI/Ti_{0.91}O_2/PEI/GO)_5$ were deposited onto PMMA spheres. Finally, the resulting product was dispersed in water by sonication and dried by lyophilization. 0.1 g of dried sample in a carbon-powder-surrounding crucible was placed inside a conventional microwave oven in an argon (Ar) atmosphere. The microwave oven (Galanz G80F20CN1L-DG (SO)) was operated at full power (800 W), 2.45 GHz, in 200 s cycles (on for 150 s, off for 50 s) for a total reaction time of 600 s. During microwave irradiation, GO was reduced to G, the PEI moiety was removed, and PMMA particles were decomposed. After reaction hollow shells consisting of alternating $Ti_{0.91}O_2$ nanosheets and G nanosheets were obtained, and trifle PMMA residue was removed with tetrahydrofuran (THF).

Characterization: XRD (ARL X'TRA, Switzerland) data were collected using a powder diffractometer with CuKa radiation (λ = 1.540562 Å). The morphology of the samples was observed by SEM (FEI NOVA NanoSEM230, USA) and TEM (JEOL 3010, Japan). FTIR spectroscopy was conducted using a Nicolet NEXUS870 (USA) spectrometer. Raman spectra were measured on a JY HR800 laser Raman spectrometer (JOBIN YVON, France) with 488 nm argon laser excitation. The PL spectra were detected at room temperature on a spectrofluorometer (VARIAN, Cary Eclipse, USA) using a 255 nm excitation wavelength at a scan speed of 600 nm min^{-1} with the PMT voltage of 650 V.

Photocatalytic Experiments: In the photocatalytic reduction of CO_2, the 0.01 g of the hollow spheres was uniformly dispersed on the glass reactor with an area of 4.2 cm^2. A 300 W xenon arc lamp was used as the light source for the photocatalytic reaction. The volume of the reaction system was about 230 mL. The reaction setup was vacuum-treated several times, and then the high purity of CO_2 gas was followed into the reaction setup for reaching ambient pressure. 0.4 mL of deionized water was injected into the reaction system as reducer. The as-prepared photocatalysts were allowed to equilibrate in the CO_2/H_2O atmosphere for several hours to ensure that the adsorption of gas molecules was complete. During the irradiation, about 0.5 mL of gas was continually taken from the reaction cell at given time intervals for subsequent CH_4 or CO concentration analysis by using a gas chromatograph (GC-2014, Shimadzu Corp., Japan). All samples were treated at 350 °C for 1 h at vacuum for removal of organic adsorbates before the photocatalysis reaction.

Acknowledgements

This work was supported by 973 Programs (No. 2011CB933303 and 2007CB613305), JST-MOST (No. 2009DFA61090), Fundamental Research Funds for the Central Universities (No. 1113020401 and 1115020405), JSPS-NSFC (No. 20811140087), NSFC (No. 20971048, 21173041 and 50732004), and the Open Research Fund of State Key Laboratory of Bioelectronics Southeast University.

Received: October 24, 2011
Revised: December 4, 2011
Published online: January 26, 2012

[1] C. N. R. Rao, A. K. Sood, K. S. Subrahmanyam, A. Govindaraj, *Angew. Chem. Int. Ed.* **2009**, *48*, 7752.
[2] S. Ghosh, I. Calizo, D. Teweldebrhan, E. P. Pokatilov, D. L. Nika, A. A. Balandin, W. Bao, F. Miao, C. N. Lau, *Appl. Phys.Lett.* **2008**, *92*, 151911.
[3] a) K. S. Novoselov, A. K. Geim, S. V. Morozov, D. Jiang, M. I. Katsnelson, I. V. Grigorieva, S. V. Dubonos, A. A. Firsov, *Nature* **2005**, *438*, 197; b) C. Gomez-Navarro, R. T. Weitz, A. M. Bittner, M. Scolari, A. Mews, M. Burghard, K. Kern, *Nano Lett.* **2007**, *7*, 3499; c) S. V. Morozov, K. S. Novoselov, M. I. Katsnelson, F. Schedin, D. C. Elias, J. A. Jaszczak, A. K. Geim, *Phys. Rev. Lett.* **2008**, *100*, 016602.
[4] C. Lee, X. Wei, J. W. Kysar, J. Hone, *Science* **2008**, *321*, 385.
[5] R. R. Nair, P. Blake, A. N. Grigorenko, K. S. Novoselov, T. J. Booth, T. Stauber, N. M. R. Peres, A. K.Geim, *Science* **2008**, *320*, 1308.
[6] M. D. Stoller, S. Park, Y. Zhu, J. An, R. S. Ruoff, *Nano Lett.* **2008**, *8*, 3498.
[7] A. R. Ranjbartoreh, B. Wang, X. P. Shen, G. X. Wang, *J. Appl. Phys.* **2011**, *109*, 014306.
[8] X. Wang, L. Zhi, K. Muellen, *Nano Lett.* **2008**, *8*, 323.
[9] Z. Liu, J. T. Robinson, X. Sun, H. Dai, *J. Am. Chem. Soc.* **2008**, *130*, 10876.
[10] Y. T. Liang, B. K. Vijayan, K. A. Gray, M. C. Hersam, *Nano Lett.* **2011**, *11*, 2865.
[11] a) Y. W. Zhu, S. Murali, M. D. Stoller, A. V. Velamakanni, R. D. Piner, R. S. Ruoff, *Carbon.* **2010**, *48*, 2106; b) H. M. A. Hassan, V. Abdelsayed, A. E. R. S. Khder, K. M. AbouZeid, J. Terner, M. S. El-Shall, S. I. Al-Resayes, A. A. El-Azhary, *J. Mater. Chem.* **2009**, *19*, 3832; c) A. Malesevic, R. Vitchev, K. Schouteden, A. Volodin, L. Zhang, G. V. Tendeloo, A. Vanhulsel, C. V. Haesendonck, *Nanotechnology* **2008**, *19*, 305604; d) Z. Luo, Y. Lu, L. A. Somers, A. T. C. Johnson, *J. Am. Chem. Soc.* **2009**, *131*, 898; e) A. Dato, V. Radmilovic, Z. Lee, J. Phillips, M. Frenklach, *Nano Lett.* **2008**, *8*, 2012; f) Z. Xu, H. Li, W. Li, G. Cao, Q. Zhang, K. Li, Q. Fu, J. Wang, *Chem. Commun.* **2011**, *47*, 1166.
[12] G. K. Mor, K. Shankar, M. Paulose, O. K. Varghese, C. A. Grimes, *Nano Lett.* **2006**, *6*, 215.
[13] J. M. Macak, M. Zlamal, J. Krysa, P. Schmuki, *Small* **2007**, *3*, 300.
[14] O. K. Varghese, M. Paulose, K. Shankar, G. K. Mor, C. A. Grimes, *J. Nanosci. Nanotechnol.* **2005**, *5*, 1158.
[15] a) S. C. Roy, O. K. Varghese, M. Paulose, C. A. Grimes, *ACS Nano* **2010**, *4*, 1259; b) M. R. Hoffmann, J. A. Moss, M. M. Baum, *Dalton Trans.* **2011**, *40*, 5151; c) V. Pradeep, I. J. D. Kubicki, H. H. Schobert, *Energy Environ. Sci.* **2009**, *2*, 745.
[16] A. L. Linsebigler, G. Q. Lu, J. T. Yates, *Chem. Rev.* **1995**, *95*, 735.
[17] D. P. Colombo, R. M. Bowman, *J. Phys. Chem.* **1996**, *100*, 18445.
[18] Y. Yu, J. C. Yu, J. G. Yu, Y. C. Kwok, Y. K. Che, J. C. Zhao, L. Ding, W. K. Ge, P. K. Wong, *Appl. Catal. A, Gen.* **2005**, *289*, 186.
[19] T. N. Lambert, C. A. Chavez, B. Hernandez-Sanchez, P. Lu, N. S. Bell, A. Ambrosini, T. Friedman, T. J. Boyle, D. R. Wheeler, D. L. Huber, *J. Phys. Chem. C.* **2009**, *113*, 19812.
[20] H. Bai, C. Li, G. Shi, *Adv. Mater.* **2011**, *23*, 1089.
[21] F. Zou, Y. A. Yu, N. Cao, L. Z. Wu, J. F. Zhi, *Scripta Mater.* **2011**, *64*, 621.
[22] G. Williams, B. Seger, P. V. Kamat, *ACS Nano* **2008**, *2*, 1487.
[23] H. B. Yao, L. H. Wu, C. H. Cui, H. Y. Fang, S. H. Yu, *J. Mater. Chem.* **2010**, *20*, 5190.
[24] B. Li, X. Zhang, X. Li, L. Wang, R. Han, B. Liu, W. Zheng, X. Li, Y. Liu, *Chem. Commun.* **2010**, *46*, 3499.
[25] a) J. Liu, H. Bai, Y. Wang, Z. Liu, X. Zhang, D. D. Sun, *Adv. Funct. Mater.* **2010**, *20*, 4175; b) N. Li, G. Liu, C. Zhen, F. Li, L. L. Zhang, H. M. Cheng, *Adv. Funct. Mater.* **2011**, *21*, 1717; c) J. T. Zhang, Z. G. Xiong, X. S. Zhao, *J. Mater. Chem.* **2011**, *21*, 3634.
[26] Y. Zhang, Z. R. Tang, X. Fu, Y. J. Xu, *ACS Nano* **2010**, *4*, 7303.

[27] H. Zhang, X. Lv, Y. Li, Y. Wang, J. Li, *ACS Nano* **2010**, *4*, 380.
[28] X. Y. Zhang, H. P. Li, X. L. Cui, Y. Lin, *J. Mater. Chem* **2010**, *20*, 2801.
[29] W. Fan, Q. Lai, Q. Zhang, Y. Wang, *J. Phys. Chem. C* **2011**, *115*, 10694.
[30] K. K. Manga, Y. Zhou, Y. Yan, K. P. Loh, *Adv. Funct. Mater.* **2009**, *19*, 3638.
[31] Y. T. Liang, B. K. Vijayan, K. A. Gray, M. C. Hersam, *Nano Lett.* **2011**, *11*, 2865.
[32] a) T. Sasaki, M. Watanabe, *J. Am. Chem. Soc.* **1998**, *120*, 4682; b) L. Wang, T. Sasaki, Y. Ebina, K. Kurashima, M. Watanabe, *Chem. Mater.* **2002**, *14*, 4827.
[33] a) J. C. Laura, K. Franklin, J. X. Huang, *J. Am. Chem. Soc.* **2009**, *131*, 1043; b) W. S. Hummers, R. E. Offeman, *J. Am. Chem. Soc.* **1958**, *80*, 1339; c) N. I. Kovtyukhova, P. J. Ollivier, B. P. Martin, T. E. Mallouk, S. A. Chizhik, E. V. Buzaneva, A. D. Gorchinskiy, *Chem. Mater.* **1999**, *11*, 771; d) D. Li, M. B. Muller, S. Gilje, R. B. Kaner, G. G. Wallace, *Nat. Nanotechnol.* **2008**, **3**, 101; e) Y. Zhou, Q. L. Bao, L. A. L. Tang, Y. L. Zhong, K. P. Loh, *Chem. Mater.* **2009**, *21*, 2950.
[34] A. C. Ferrari, *Solid State Commun.* **2007**, *143*, 47.
[35] K. N. Kudin, B. Ozbas, H. C. Schniepp, R. K. Prud'homme, I. A. Aksay, R. Car, *Nano Lett.* **2008**, *8*, 36.
[36] a) E. J. Tang, G. X. Cheng, X. L. Ma, *Powder Technol.* **2006**, *161*, 209; b) K. Moller, T. Bein, R. X. Fischer, *Chem. Mater.* **1998**, *10*, 1841.
[37] T. F. Yeh, J. M. Syu, C. Cheng, T. H. Chang, H. S. Teng, *Adv. Funct. Mater.* **2010**, *20*, 2255.
[38] J. J. Guo, S. M. Zhu, Z. X. Chen, Y. Li, Z. Y. Yu, Q. L. Liu, J. B. Li, C. L. Feng, D. Zhang, *Ultrason. Sonochem.* **2011**, *18*, 1082.
[39] a) T. Yui, A. Kan, C. Saitoh, K. Koike, T. Ibusuki, O. Ishitani, *ACS Appl. Mater. Interface* **2011**, *3*, 2594; b) G. Dey, *J. Nat. Gas Chem.* **2007**, *16*, 217.
[40] T. Sasaki, M. Watanabe, *J. Phys. Chem. B* **1997**, *101*, 10159.
[41] G. Liu, L. Wang, H. G. Yang, H. M. Cheng, G. Q. Lu, *J. Mater. Chem.* **2010**, *20*, 831.